Dynamic Modelling and Payload Response Analysis of a 3-D Overhead Gantry Crane

Aakash Krishna, Ravindra Singh Bisht, and Soraj Kumar Panigrahi

1 Introduction

Crane systems are commonly used at civil construction sites, warehouses, manufacturing plants, and port facilities to handle various types of payloads. The crane system helps the industry for transporting various payloads from one place to another. Industry uses various popular cranes such as truck-mounted crane, tower crane, gantry crane, rough-terrain crane, and port crane. These cranes may be classified as per their dynamic properties according to various coordinate systems. At high-rise construction sites, generally, a tower crane is used, and a cylindrical coordinate system is used to describe the mathematical modelling for movement of the payload during the crane operation. The payload is supported by wire hoist, and the trolley moves along the boom arm in case of a gantry crane. The gantry crane uses a Cartesian space to describe the position and movement of the system. The port/boom crane is used as a spherical coordinate to describe the movement of the system. The payload is backed by the wire rope suspension. A port crane is normally placed on a base to facilitate the change of the workspace. All types of crane systems must work very quickly, safely, and precisely, because efficiency is directly related to the productivity of material handling in industries. Industry uses double-pendulum [1–11] suspension-type cranes where both the hook and the payload are subjected to dynamic excitation.

A double-pendulum crane system represents the motion of both the hook and payload. The operation of the crane system becomes extremely difficult due to the nonlinear dynamic behaviour of the double pendulum [11–15] particularly when the

A. Krishna
Quantum School of Technology, Roorkee 247667, India

R. S. Bisht (✉) · S. K. Panigrahi
CSIR-Central Building Research Institute Roorkee, Roorkee 247667, India
e-mail: rsbisht@cbri.res.in

V. H. Saran and R. K. Misra (eds.), *Advances in Systems Engineering*,
Lecture Notes in Mechanical Engineering,
https://doi.org/10.1007/978-981-15-8025-3_19

crane base or rail and trolley of the crane is movable. The overhead crane system based on the assumption of a unique pendulum model is not always true. In some cases, the mass of the hook cannot be ignored, which has led to a double pendulum-type system [8, 9]. Unlike a simple pendulum that only balances the payload, a double pendulum must take into account the balancing of the payload and the balancing of the hook. It has been reported that a double-pendulum crane underwent oscillations of the payload [1–4, 10–15] and its effective control strategies [1, 2, 5–9, 12, 13, 16, 17]. Therefore, designing a precise, safe, and fast-operated double-pendulum crane system to position the load with minimum payload swing is more challenging due to the complexity and chaotic dynamic behaviour of the double pendulum.

This study presents the mathematical modelling of a three-dimensional (3-D) gantry crane with a double-pendulum dynamics. The dynamic equations are derived using the Lagrangian approach. Subsequently, the output payload response is determined in time and frequency domain by developing algorithms in MATLAB for better crane payload swing control. This paper is divided into four sections. The first section gives a brief overview of the problem. The second section deals with the physical model and parameters of the gantry crane. The 3-D gantry crane mathematical modelling is described in the third section. The fourth section presents results and discussion of the key findings. Conclusions are drawn in the final section.

2 Physical Model Representation of the Gantry Crane System

The physical model of the overhead gantry system shown in Fig. 1 incorporates its motion in 3-D space including double-pendulum motion, where an external driving force ($F \in \mathrm{R}^2$) moves the trolley and rail simultaneously. The gantry crane system comprises four subsystems. i.e., rail for X-axis movement, trolley for Y-axis movement, a combination of hook and payload where θ_1 and φ_1 are the hook rope swing angles; θ_2 and φ_2 is the payload rope swing angles; L_1 and L_2 are the wire rope length of hook and payload, respectively.

The hook ball mass moment of inertia (j_h) is assumed constant [14]; however, the payload ball mass moment (j_p) of inertia is varying according to variations in the payloads (m_p). For simplified mathematical modelling, the rail and trolley-wheel friction force and the flexibility of the wire rope are neglected. The physical parameters of the gantry crane [15, 18] are given in Table 1.

3 Mathematical Modelling

The total kinetic and potential energy associated with the gantry crane needs to be derived, and then, the Lagrangian formulation for dynamic modelling is used to

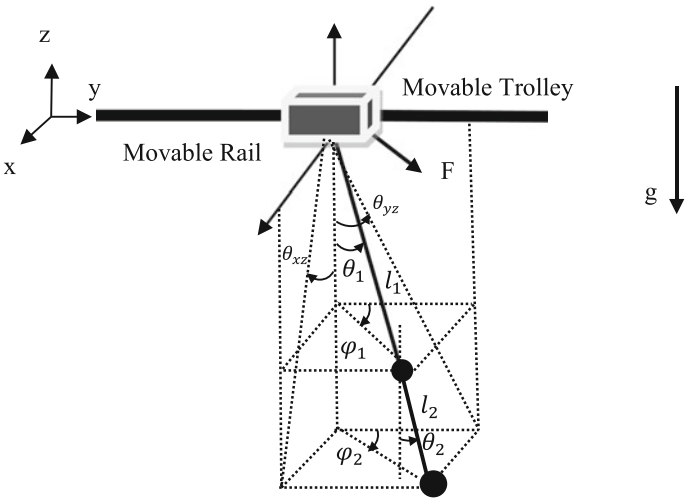

Fig. 1 Mathematical representation of the 3-D gantry crane using a double-pendulum modelling approach

Table 1 Parameters of the crane system

Parameter	Trolley mass	Rail mass	Hook ball mass	Payload ball mass	Hook moment of inertia	Payload moment of inertia	Hook rope length	Payload rope length
Symbol	m_t	m_r	m_h	m_p	j_h	j_p	l_1	l_2
Value	1.06 kg	6.4 kg	0.1 kg	Variable	0.005 kg-m^2	Variable	2.0 m	1.0 m

derive the 3-D gantry crane overall system response. Simulation is performed using a state-space model of the gantry crane by MATLAB ode45 solver.

3.1 Kinetic Energy

The rail, trolley, hook, and payload position vectors are derived using Fig. 1. The position vectors are $r_r = [x, 0, 0]^T, r_t == [x, y, 0]^T$, $r_h = [x + L_1 \sin\theta_1 \sin\varphi_1, y + L_1 \sin\theta_1 \cos\varphi_1, -L_1 \cos\theta_1]^T$, and $r_p = [x + L_1 \sin\theta_1 \sin\varphi_1 + L_2 \sin\theta_2 \sin\varphi_2, y + L_1 \sin\theta_1 \cos\varphi_1 + L_2 \sin\theta_2 \cos\varphi_2, -L_1 \cos\theta_1 - L_2 \cos\theta_2]^T$, respectively, where the trolley positions in X- and Y-directions are represented by parameters x and y, respectively. The kinetic energy, KE, of the whole crane system is given in Eq. (1),

$$\mathrm{KE} = k_{\mathrm{rail}} + k_{\mathrm{trolley}} + k_{\mathrm{hook}} + k_{\mathrm{payload}} \tag{1}$$

where $k_{\text{rail}} = \frac{1}{2}m_r\dot{r}_r^2$, $k_{\text{trolley}} = \frac{1}{2}m_t\dot{r}_t^2$, $k_{\text{hook}} = \frac{1}{2}m_h\dot{r}_h^2 + \frac{1}{2}J_h\dot{\theta}_1^2 + \frac{1}{2}J_h\dot{\varphi}_1^2$, $k_{\text{payload}} = \frac{1}{2}m_p\dot{r}_p^2 + \frac{1}{2}J_p\dot{\theta}_2^2 + \frac{1}{2}J_p\dot{\varphi}_2^2$.

3.2 Potential Energy

The total potential energy, PE, of the whole crane system is given in Eq. (2),

$$\text{PE} = p_{\text{hook}} + p_{\text{payload}} \tag{2}$$

where $p_{\text{hook}} = -m_h g L_1 \cos\theta_1$, $p_{\text{payload}} = -m_p g(L_1 \cos\theta_1 + L_2 \cos\theta_2)$ and g is the gravity acceleration vector.

3.3 Lagrangian Formulation

The Lagrangian approach as shown in Eq. (3) is used to derive the system equations of motion for dynamic response analysis.

$$\frac{\mathrm{d}}{\mathrm{d}t}\left(\frac{\partial L}{\partial \dot{q}_i}\right) - \frac{\partial L}{\partial q_i} = F_i, \qquad i = 1, \ldots, 6 \tag{3}$$

where $L(q, \dot{q}) = \text{KE} - \text{PE}$, $q(t) = \left[x\ y\ \theta_1\varphi_1\theta_2\varphi_2\right]^T$ is the state vector and $F = \left[F_x F_y 0000\right]^T$ is the input excitation force vector, which is defined by a bang–bang control signal where F_x and F_y denote the input control force acting on the trolley along with the X- and Y-axis directions.

From Eq. (3), the dynamic model of the crane system is then expressed in the form of matrices for further conversion in the state-space representation of dynamic payload simulations.

$$M(q)\ddot{q} + V(q, \dot{q}) + G(q) = F(t) \tag{4}$$

The system response can be expressed in the following form of the equation of motions from Eq. (4).

$$\ddot{q}(t) = M(q)^{-1}(-V(q, \dot{q}) - G(q) + F(t)) \tag{5}$$

where in the above Eq. (5), the matrices $M(q) \in R^{6\times6}$, $V(q, \dot{q}) \in R^{6\times1}$, and $G(q) \in R^{6\times1}$ represent the Inertia, Centripetal–Coriolis, and gravity terms, respectively, and these matrices terms are further defined in the given appendix.

4 Results and Discussions

For swing and motion response of the payload analysis, the trolley of the gantry crane is excited using a bang–bang signal of amplitude 2 *N* force along the *X*-axis and 1 *N* of force along the *Y*-axis. The applied force signal is represented in Fig. 2. The bang–bang force signal has equal acceleration and deceleration periods. Some examples of the used bang–bang signal for payload response simulation can be found elsewhere [15, 18].

Simulation steps using developed algorithms for swing and motion responses of the payload analysis in both time and frequency domain are shown in Fig. 3.

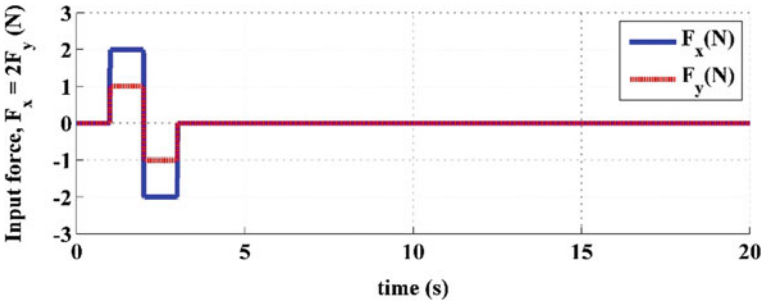

Fig. 2 Input force excitation applied on the trolley for dynamic payload response

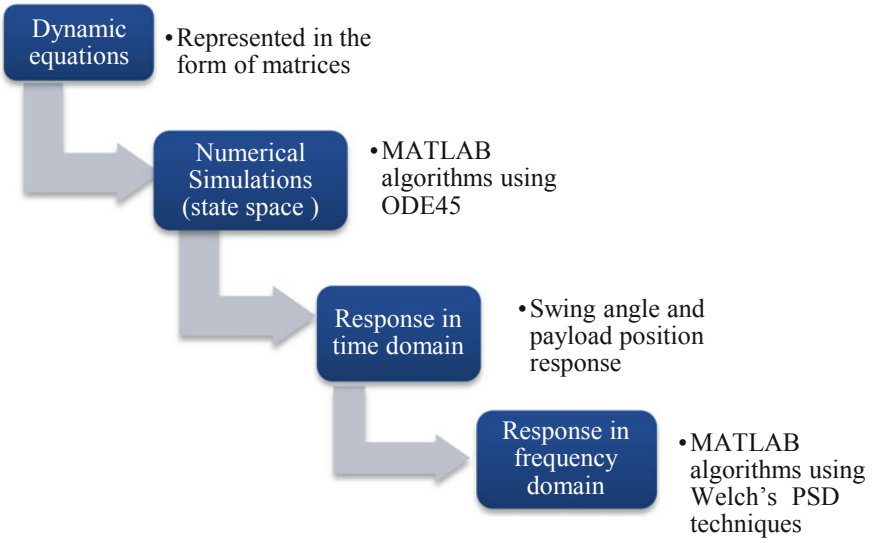

Fig. 3 Simulation steps using the developed algorithms for dynamic response analysis

The results given in Fig. 4 show the payload swing angle response (θ_{yz} and θ_{xz}) with respect to *XZ* and *YZ* planes with the various mass (m_p) of the payload. It shows that the oscillation of the swing angles decreases with increasing mass (m_p) of the payload. For other cases, in the simulation, if we increase the hook rope length (l_1), the swing angles also increase.

Simulation results in Fig. 5a and b show the variation of time response along *X*-, *Y*-, and *Z*-axis in 3D space of the payload motion with the variation of payloads mass. It shows that the amplitude of the *X*-, *Y*-, and *Z*-axis oscillation of the payload decreases with increasing mass of the payload. It is more visible when we see the 3-D phase plot of the payload amplitude oscillations shown in Fig. 5b. It is observed from Fig. 5b that when the mass of payload increases, the amplitude of the response decreases.

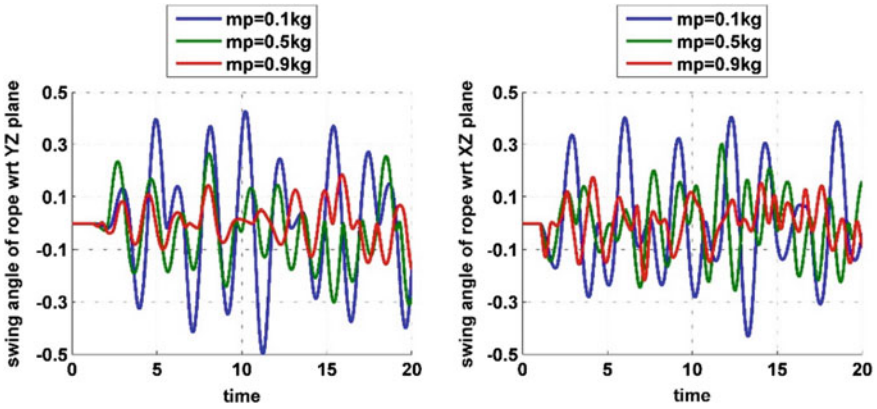

Fig. 4 Dynamic response of the payload swing angles (rad.) versus time (s)

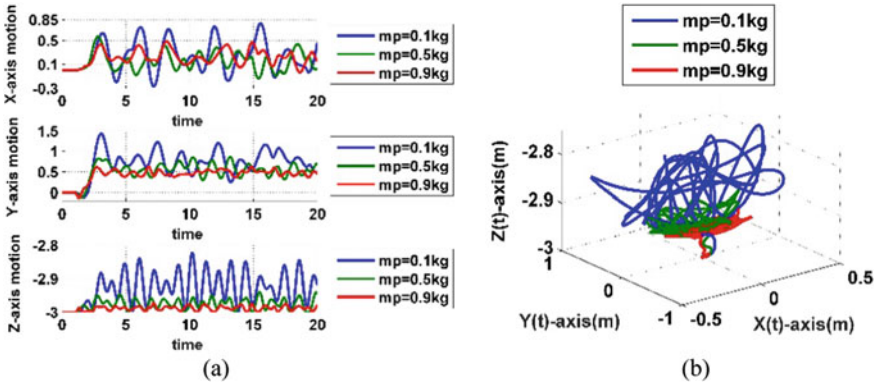

Fig. 5 Dynamic response of the payload, **a** time response plot, displacement (m) versus time (s), **b** 3-D phase response plot

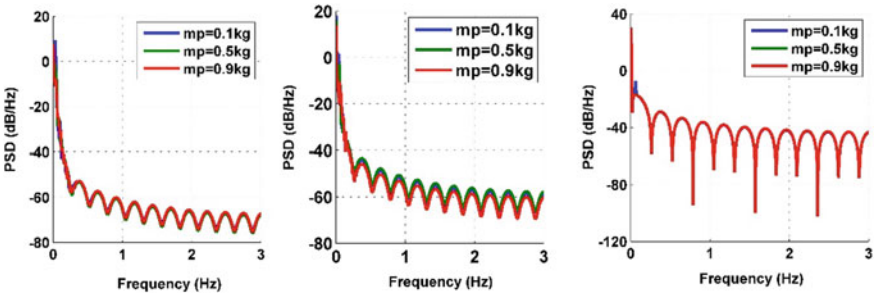

Fig. 6 Power spectral density of *X*, *Y*, and *Z* payload dynamic response

Table 2 Frequencies of payload response along the *X*-, *Y*-, and *Z*-axis for the first two modes

Payload (kg)	Resonance frequency (Hz)					
	Payload response *X*-axis		Payload response *Y*-axis		Payload response *Z*-axis	
	Mode-1	Mode-2	Mode-1	Mode-2	Mode-1	Mode-2
0.1	0.024	0.360	0.036	0.640	0.061	0.660
0.5	0.030	0.374	0.049	0.645	0.062	0.660
0.9	0.042	0.380	0.055	0.650	0.067	0.660

After knowing the dynamic response of the payload along *X*-, *Y*-, and *Z*-axis in 3-D space, the power spectral density (PSD) is then compared and evaluated using MATLAB algorithms. It is observed from Fig. 6 that the higher the payload mass, the resonance frequency is also higher, and there is not much frequency variation for higher modes of vibration. The resonance frequencies for the first two modes and payloads relation is summarized in Table 2.

5 Conclusion

In the present study, a 3-D gantry crane system considering double-pendulum effect due to hook and payload has been modelled, and payload response simulation is performed. Lagrange approach has been used to develop the system equations of motion. Bang–bang force input is used to simulate the gantry crane payload dynamic response behaviour. The crane payload position in 3-D space and swing angle responses have been obtained using the developed dynamic modelling, and further analysis is performed both in time and frequency domains by developing MATLAB algorithms. The influence of the parameters such as payload mass and hook rope length variations has been considered in the gantry crane system dynamic study and simulation. These dynamic response study may be further useful for effective payload response control of gantry cranes with varying system parameters. This

study presented on the dynamics of 3-D gantry crane may also be useful for studying the dynamic behaviour and control strategies of other types of mobile crane systems.

Acknowledgements The work presented in the paper is the output of a CSIR, India, sponsored R&D project on Mass Housing Development (HCP-015).

Appendix

$$M(q) = \begin{bmatrix} m_{11} & m_{12} & m_{13} & m_{14} & m_{15} & m_{16} \\ m_{21} & m_{22} & m_{23} & m_{24} & m_{25} & m_{26} \\ m_{31} & m_{32} & m_{33} & m_{34} & m_{35} & m_{36} \\ m_{41} & m_{42} & m_{43} & m_{44} & m_{45} & m_{46} \\ m_{51} & m_{52} & m_{53} & m_{54} & m_{55} & m_{56} \\ m_{61} & m_{62} & m_{63} & m_{64} & m_{65} & m_{66} \end{bmatrix}$$

$m_{11} = m_h + m_p + m_r + m_t,$
$m_{12} = m_{21} = 0,$
$m_{13} = m_{31} = L_1 \cos\theta_1 \sin\varphi_1 m_h + L_1 \cos\theta_1 \sin\varphi_1 m_p,$
$m_{14} = m_{41} = L_1 \sin\theta_1 \cos\varphi_1 m_h + m_p L_1 \sin\theta_1 \cos\varphi_1$
$m_{15} = m_{51} = L_2 \sin\varphi_2 \cos\theta_2 m_p,$
$m_{16} = m_{61} = L_1 \sin\theta_2 \cos\varphi_2 m_p,$
$m_{22} = m_h + m_p + m_t,$
$m_{23} = m_{32} = L_1 \cos\varphi_1 \cos\theta_1 m_h + L_1 \cos\varphi_1 \sin\theta_2 m_p,$
$m_{24} = m_{42} = -L_1 \sin\theta_1 \sin\varphi_1 m_h - m_p L_1 \sin\varphi_1 \sin\theta_1,$
$m_{25} = m_{52} = L_2 \cos\varphi_2 \cos\theta_2 m_p,$
$m_{26} = m_{62} = -L_1 \sin\varphi_2 \sin\varphi_2 m_p,$
$m_{31} = L_1 \cos\theta_1 \sin\varphi_1 m_h + L_1 \cos\theta_1 \sin\varphi_1 m_p,$
$m_{32} = L_1 \cos\varphi_1 \cos\theta_1 m_h + L_1 \cos\theta_1 \cos\varphi_1 m_p,$
$m_{33} = m_h L_1^2 + m_p L_1^2 + J_h,$
$m_{34} = m_{43} = m_{35} = m_{53} = m_{36} = m_{63} = 0,$
$m_{44} = -L_1^2 \cos^2\theta_1 m_h - L_1^2 \cos\theta_1^2 m_p + m_h L_1^2 + m_p L_1^2 + J_h,$
$m_{45} = m_{54} = m_{46} = m_{64} = 0,$
$m_{55} = m_p L_2^2 + J_p, m_{56} = m_{65} = 0,$
$m_{66} = m_p L_2^2 + J_p - L_1^2 \cos\theta_2^2 m_p$

$$V(q, \dot{q}) = \begin{bmatrix} V_{11} \\ V_{21} \\ V_{31} \\ V_{41} \\ V_{51} \\ V_{61} \end{bmatrix},$$

$$
\begin{aligned}
V_{11} &= -L_1 \sin\varphi_1 \dot{\theta}_1^2 \sin\theta_1 m_h - L_1 \sin\varphi_1 \dot{\theta}_1^2 \sin\theta_1 m_p \\
&\quad + 2L_1 \cos\varphi_1 \dot{\varphi}_1 \dot{\theta}_1 \cos\theta_1 m_h + 2L_1 \cos\varphi_1 \dot{\varphi}_1 \dot{\theta}_1 \cos\theta_1 m_p \\
&\quad - L_1 \sin\varphi_1 \dot{\varphi}_1^2 \sin\theta_1 m_h - L_1 \sin\varphi_1 \dot{\varphi}_1^2 \sin\theta_1 m_p - L_2 \sin\varphi_2 \dot{\theta}_2^2 \sin\theta_2 m_p \\
&\quad + 2L_2 \cos\varphi_2 \dot{\varphi}_2 \dot{\theta}_2 \cos\theta_2 m_p - L_2 \sin\varphi_2 \varphi_2^2 \sin\theta_2 m_p, \\
V_{21} &= -2L_1 \sin\varphi_1 \dot{\varphi}_1 \cos\theta_1 \dot{\theta}_1 m_h - 2L_1 \sin\varphi_1 \dot{\varphi}_1 \dot{\theta}_1 \cos\theta_1 m_p \\
&\quad - L_1 \cos\varphi_1 \dot{\theta}_1^2 \sin\theta_1 m_h \\
&\quad - L_1 \cos\varphi_1 \dot{\theta}_1^2 \sin\theta_1 m_p - L_1 \cos\varphi_1 \dot{\varphi}_1^2 \sin\theta_1 m_h \\
&\quad - L_1 \cos\varphi_1 \dot{\varphi}_1^2 \sin\theta_1 m_p \\
&\quad - 2L_2 \sin\varphi_2 \dot{\varphi}_2 \dot{\theta}_2 \cos\theta_2 m_p - L_2 \cos\varphi_2 \dot{\theta}_2^2 \sin\theta_2 m_p \\
&\quad - L_2 \cos\varphi_2 \dot{\varphi}_2^2 \sin\theta_2 m_p \\
V_{31} &= -\dot{\varphi}_1^2 L_1^2 \cos\theta_1 \sin\theta_1 \left(m_h + m_p\right), \\
V_{41} &= 2L_1^2 \cos\theta_1 m_h \sin\theta_1 \dot{\varphi}_1 \dot{\theta}_1 \left(m_h + m_p\right), \\
V_{51} &= -L_2^2 \cos\theta_2 m_p \sin\theta_2 \dot{\varphi}_2^2,\ V_{61} = 2L_2^2 \cos\theta_2 m_p \sin\theta_2 \dot{\varphi}_2 \dot{\theta}_2
\end{aligned}
$$

$$
G(q) = \begin{bmatrix} 0 \\ 0 \\ m_h g L_1 \sin\theta_1 + m_p g L_1 \sin\theta_1 \\ 0 \\ m_p g L_2 \sin\theta_2 \\ 0 \end{bmatrix}.
$$

References

1. Karajgikar A, Vaughan J, Singhose W (2011) Double-pendulum crane operator performance comparing pd-feedback control and input shaping. In: Proceedings of the ECCOMAS thematic conference on advances in computational multibody dynamics, Brussels, Belgium, pp 1–14
2. Qian D, Tong S, Yang B, Lee S (2015) Design of simultaneous input-shaping-based SIRMs fuzzy control for double pendulum-type overhead cranes. Bull Pol Acad Sci Tech Sci 63(4):887–896
3. Weiping G, Diantong L, Jianqiang Y, Dongbin Z (2004) Passivity-based-control for double-pendulum-type overhead cranes. In: IEEE region 10 conference TENCON 2004, pp 546–549
4. Kenison M, Singhose W (1999) Input shaper design for double-pendulum planar gantry cranes. In: Proceedings of the 1999 IEEE international conference on control applications, Hawaii, USA, pp 539–544
5. Vaughan J, Maleki E, Singhose W (2010) Advantages of using command shaping over feedback for crane control. In: Proceedings of the 2010 american control conference, Baltimore, USA, pp 2308–2313
6. Zhang M, Ma X, Rong M, Tian X, Li Y (2016) Adaptive tracking control for double-pendulum overhead cranes subject to tracking error limitation, parametric uncertainties and external disturbances. Mech Syst Signal Process 76:15–32
7. Vaughan J, Kim D, Singhose W (2010) Control of tower cranes with double-pendulum payload dynamics. IEEE Trans Control Syst Technol 18(6):1345–1358

8. Qian D, Tong S, Lee S (2016) Fuzzy-logic-based control of payloads subjected to double-pendulum motion in overhead cranes. Automa Constr 65:133–143
9. Kim D, Singhose W (2010) Performance studies of human operators driving double-pendulum bridge cranes. Control Eng Pract 18(6):567–576
10. Ahmad MA, Raja Ismail RMT, Ramli MS, Hambali N (2010) Investigations of NCTF with input shaping for sway control of a double-pendulum-type overhead crane. In: International conference on advanced computer control, Shenyang, China, pp 456–461
11. Huang J, Liang Z, Zang Q (2015) Dynamics and swing control of double-pendulum bridge cranes with distributed-mass beams. Mech Syst Signal Process 54–55:357–366
12. Kim D, Singhose W (2006) Reduction of double-pendulum bridge crane oscillations. In: The 8th international conference on motion and vibration control (MOVIC 2006), 27–30 August, Daejeon, Korea, pp 300–305
13. Singhose WE, Towell ST (1998) Double-pendulum gantry crane dynamics and control. In: Proceedings of the 1998 IEEE international conference on control applications, Trieste, pp 1205–1209
14. Chang CY, Chiang KH (2008) Fuzzy projection control law and its application to the overhead crane. Mechatronics 18(10):607–615
15. Ismail RMTR, Ahmad MA, Ramli MS, Rashidi FRM (2009) Nonlinear dynamic modelling and analysis of a 3-D overhead gantry crane system with payload variation. In: 2009 Third UKSim European symposium on computer modeling and simulation. IEEE, pp 350–354
16. Singhose W, Kim D, Kenison M (2008) Input shaping control of double-pendulum bridge crane oscillations. J Dyn Syst Meas Contr 130(3):034504
17. O'Connor W, Habibi H (2013) Gantry crane control of a double-pendulum, distributed-mass load, using mechanical wave concepts. Mech Sci 4:251–261
18. Ismail RMTR, Ahmad MA, Ramli MS, Ishak R, Zawawi MA (2011) Dynamic modelling of a double-pendulum gantry crane system incorporating payload. AIP Conf Proc 1337(1):118–122